MOLECULAR AND CELLULAR BIOLOGY, Mar. 2008, p. 1713–1723 Vol. 28, No. 5
0270-7306/08/$08.00+0 doi:10.1128/MCB.01360-07

β-Catenin Expression Results in p53-Independent DNA Damage and Oncogene-Induced Senescence in Prelymphomagenic Thymocytes In Vivo▽†

Mai Xu,[1] Qing Yu,[1] Ramesh Subrahmanyam,[2] Michael J. Difilippantonio,[3] Thomas Ried,[3] and Jyoti Misra Sen[1]*

Lymphocyte Development Unit, Laboratory of Immunology,[1] and Laboratory of Cellular and Molecular Biology,[2] National Institute on Aging, Baltimore, Maryland 21224, and Section of Cancer Genomics, Genetics Branch, National Cancer Institute, National Institutes of Health, Bethesda, Maryland 20892[3]

Received 28 August 2008/Returned for modification 22 October 2007/Accepted 11 December 2007

The expression of β-catenin, a potent oncogene, is causally linked to tumorigenesis. Therefore, it was surprising that the transgenic expression of oncogenic β-catenin in thymocytes resulted in thymic involution instead of lymphomagenesis. In this report, we demonstrate that this is because the expression of oncogenic β-catenin induces DNA damage, growth arrest, oncogene-induced senescence (OIS), and apoptosis of immature thymocytes. In p53-deficient mice, the expression of oncogenic β-catenin still results in DNA damage and OIS, but the thymocytes survive and eventually progress to thymic lymphoma. β-Catenin-induced thymic lymphomas are distinct from lymphomas that arise in $p53^{-/-}$ mice. They are $CD4^-$ $CD8^-$, while p53-dependent lymphomas are largely $CD4^+$ $CD8^+$, and they develop at an earlier age and in the absence of c-Myc expression or Notch1 signaling. Thus, we report that oncogenic β-catenin-induced, p53-independent growth arrest and OIS and p53-dependent apoptosis protect developing thymocytes from transformation by oncogenic β-catenin.

Cells sense and respond to their environment via signaling cascades initiated at the cell surface. These signals are propagated by various mechanisms through the cytoplasm, ultimately resulting in the alteration of gene expression patterns in the nucleus. One such pathway is the canonical Wnt–β-catenin–T-cell factor (TCF) pathway, which plays a causative role in cancers of the colon (17, 23, 25, 28, 61), breast (37, 48), and epidermal (18, 26, 43) tissues. Accordingly, tissue-specific expression of transgenic β-catenin can result in the development of aggressive tumors early in life (13, 23, 34). Briefly, the secreted extracellular Wnt glycoproteins bind to the Frizzled receptors on the surface of cells. This results in the release of β-catenin from a destruction complex, allowing it to accumulate in the cytoplasm. β-Catenin then travels to the nucleus, where it binds to the transcription factors TCF/lymphocyte enhancer binding factor to activate the transcription of target genes linked to cellular proliferation and cancer, including c-*Myc* and *cyclin D1* (25, 61). Cancers involving stabilized β-catenin often deregulate the tumor suppressor *p53*, whose function normally impedes tumor formation by inducing growth arrest or apoptosis (24, 28). Thus, p53 appears to be an important impediment to β-catenin-induced tumorigenesis; however, the molecular mechanisms remain poorly understood.

In the thymus, T-cell development is characterized by the expression of the cell surface markers CD4 and CD8 in the following order: double-negative cells (DN), double-positive cells (DP), and either CD4- or CD8-expressing single-positive (SP) cells that migrate out of the thymus into the periphery. The DN population is further divided into four subpopulations based on the cell surface expression of CD44 and/or CD25 into DN1, DN2, DN3, and DN4. At the DN2 and DN3 stages of development, thymocytes undergo RAG-dependent V(D)J rearrangements to generate the recombined T-cell receptor (TCR) β-chain. The generation of double-stranded breaks (DSBs) during V(D)J recombination is tightly coupled to the recruitment of the efficient nonhomologous end-joining (NHEJ) repair machinery in order to minimize DNA damage and aberrant repair (4, 30) and to p53-dependent growth arrest and the apoptotic removal of irreparably damaged cells (19, 22). Therefore, only a small fraction of NHEJ mutant mice develop tumors after a long latency of at least 6 months (9, 31, 50). Cell surface expression of the TCRβ chain in conjunction with a nonrearranging pre-Tα chain allows for β-selection (63). This consists of cell survival signals, a burst of proliferative activity, and progression through the DN4 stage to the DP stage of development, where recombination at the TCRα locus occurs (12, 14). Despite vulnerability to DSBs from specific RAG-dependent events and from proliferative bursts, thymocytes efficiently escape transformation. However, the mechanisms that protect developing thymocytes from transformation during development remain unknown.

The Wnt/β-catenin/TCF pathway has been implicated in multiple stages of hematopoietic development, including the self-renewal of hematopoietic stem cells (47) and their development to multiple lineages (29, 52). In the thymus, a double deletion of Wnt1 and Wnt4 results in significantly reduced thymic cellularity (39). The loss of the transcription factor TCF

* Corresponding author. Mailing address: Lymphocyte Development Unit, Laboratory of Immunology, National Institute on Aging, 5600 Nathan Shock Drive, Room 4B08 GRC, Baltimore, MD 21224. Phone: (410) 558-8163. Fax: (410) 558-8284. E-mail: Jyoti-Sen@nih.gov.

† Supplemental material for this article may be found at http://mcb.asm.org/.

▽ Published ahead of print on 26 December 2007.

impairs the development of DN thymocytes (53), and a double deletion of TCF and lymphocyte enhancer binding factor impedes thymocyte development (42). The expression of soluble Frizzled, Dickkopf, or ICAT, all inhibitors of the Wnt signaling pathway, blocks the development of T-cell precursors in in vitro assays (45, 59). The T-cell-specific deletion of β-catenin results in a developmental block at the DN3-to-DN4 stage and in the reduced proliferation of DN4 thymocytes (65). Conversely, the dramatic overexpression of β-catenin permits the maturation of DN thymocytes to the DP stage, in a RAG-deficient background, without expression of the TCRβ chain or proliferation (15, 16). Indeed, the enforced expression of β-catenin in DP thymocytes induces c-Myc-dependent DP lymphomas (20). In contrast, the modest transgenic expression of β-catenin in developing thymocytes enhances the generation of CD8 SP thymocytes and accelerates thymic involution (40, 66). Since endogenous β-catenin expression is regulated by intrathymic signals and plays essential roles in cell survival and proliferation during normal T-cell development, the deregulated expression of β-catenin might be expected to result in the development of thymic lymphomas.

The expression of oncogenes, contrary to expectation, can trigger a permanent block in replication. This inability of cells to divide was termed oncogene-induced senescence (OIS) (55). OIS has been shown to restrict the growth of human and murine precancerous tissues (2, 5, 6, 38, 56). Other studies have shown that oncogene expression induced cellular senescence that was dependent on the expression of specific genes (2, 5). For instance, senescence triggered by the expression of oncogenic Ras in human fibroblasts resulted from the activation of DNA damage checkpoint response genes, and blocking this response resulted in cellular transformation. Furthermore, in vivo DNA labeling and molecular DNA combing studies showed that oncogene activation led to an increased number of active replicons and altered DNA replication fork progression (10). DNA replication stress was also shown to result in prematurely terminated DNA replication forks and DNA double-strand breaks and OIS in human diploid fibroblasts (1). It remains unknown, however, whether OIS plays a role in tumor suppression during normal tissue development in vivo. Such a mechanism could be essential where the expression of oncogenes is an integral part of signaling events during tissue development, and inappropriate activation could lead to uncontrolled growth, especially in self-renewing tissues such as the thymus, where replicative bursts are required to obtain adequate cellularity throughout a lifetime.

We have previously shown that the transgenic expression of oncogenic β-catenin in the thymus results in thymic involution rather than thymic lymphomas in CAT-Tg mice (66), suggesting that thymocytes respond to oncogenic β-catenin differently than colon, mammary, and epidermal tissues in which cancer developed. Since the overexpression of β-catenin results in tumor development in other tissues, we wondered why thymocytes do not respond in a similar manner. The lack of T-cell lymphomas in CAT-Tg mice was consistent with the absence of a documented role for β-catenin in human T-cell lymphomas (44, 54). In this report, we demonstrate that the expression of oncogenic β-catenin in thymocytes at developmental stages that coincide with DNA recombination and a burst of proliferation induces DNA damage, growth arrest, and OIS in vivo. This is followed by p53-dependent apoptosis. Thus, β-catenin-dependent OIS forms an initial p53-independent barrier to thymic lymphoma formation. Together, these data indicate that both p53-independent and p53-dependent mechanisms prevent β-catenin-induced thymic lymphomas in mice. Finally, these studies also show for the first time that enhanced DNA damage signaling may be linked to OIS in normally maturing tissues in vivo.

MATERIALS AND METHODS

Mouse strains. CAT-Tg mice (40, 66) and $p53^{-/-}$ mice (Jackson laboratory) are on a C57BL/6 genetic background. Where not specified, age-matched C57BL/6 and $p53^{+/-}$, $p53^{-/-}$, and CAT-Tg littermate mice were used. Time to death was defined as the time between birth and natural death or a terminal disease stage. To obtain data for the Kaplan-Meier plot, a cohort of mice was set aside along with matched controls, and the time between birth and natural death was documented. Median time to death is when half the mice in the cohort had died. All animal procedures were in compliance with the guidelines of the National Institute on Aging animal resources facility, which operates under the regulatory requirements of the U.S. Department of Agriculture and the Association for Assessment and Accreditation of Laboratory Animal Care.

Flow cytometry and antibodies. Four-color flow cytometry was done using a FACSCalibur apparatus (BD Pharmingen). The following antibodies were purchased from BD Pharmingen: anti-CD3 conjugated to fluorescein isothiocyanate (FITC); anti-CD4 conjugated to allophycocyanin (APC), phycoerythrin (PE), or biotin; anti-CD8 conjugated to FITC, PE, peridinin chlorophyll protein-Cy5.5, or biotin; anti-c-kit conjugated to APC or PE; anti-CD25 conjugated to APC or peridinin chlorophyll protein-Cy5.5; and FITC- or PE-conjugated antibodies to TCRβ, TCRγδ, B220, Gr1, Mac1, Ter119, or NK1.1. Anti-β-catenin was purchased from BD Transduction Laboratories. Assays using the FITC-annexin V labeling kit (Roche) and a bromodeoxyuridine (BrdU) flow kit (BD Pharmingen) were performed according to the manufacturer's instructions. Briefly, 100 μl of 10 mg/ml of the BrdU solution was injected intraperitoneally. BrdU incorporation was assayed 2 h postinjection. Thymocytes were first stained with surface markers, which was followed by intracellular staining with anti-BrdU antibody. For the apoptosis assay, freshly isolated thymocytes were first stained with surface markers, which was followed by staining with FITC-conjugated annexin V. For analysis of DN thymocytes, lineage-positive cells were gated out using a cocktail of lineage-specific antibodies to CD4, CD8, TCRβ, TCRγδ, B220, NK1.1, Gr1, and Mac-1. For cell sorting, total thymocytes were stained with biotinylated anti-CD4 and anti-CD8 antibodies, followed by incubation with anti-biotin microbeads (Miltenyi) and the magnetic depletion of DP and SP cells. Enriched cell suspensions were surface stained with anti-CD25, anti-c-kit, and lineage-specific antibody cocktail, followed by sorting using MoFlo.

Quantitative and semiquantitative PCR. mRNA from sorted cells was extracted with an RNeasy Micro kit (Qiagen). cDNA was prepared with a Superscript II reverse transcriptase (RT) kit (Invitrogen). SYBR green quantitative RT-PCR was performed using PCR Master Mix from Applied Biosystems. Calculations were done according to standard methods. The expression of the target gene was determined relative to glyceraldehyde-3-phosphate dehydrogenase (GAPDH) and calculated as $2^{-(CT_{\text{target gene}} - CT_{\text{GAPDH}})}$. All primer sequences are available upon request.

Western blot analysis and immunofluorescence. Immunoblotting was performed with whole-cell lysates resolved on 4 to 12% Bis-Tris sodium dodecyl sulfate-polyacrylamide gels and detected using antibodies against mouse β-catenin (BD Transduction Laboratory), mouse α-tubulin (Sigma), and mouse PKCμ (Santa Cruz). For immunofluorescence staining, cells were deposited onto poly-lysine-precoated coverslips and fixed with methanol-acetone, followed by incubation with primary antibody against γ-H2AX (Upstate) and secondary anti-mouse immunoglobulin G antibody (Alexa Fluor 594; Molecular Probes). The coverslips were sealed with mounting medium containing DAPI (4′,6′-diamidino-2-phenylindole) before microscopy was performed by using a Zeiss Axiovert 200 microscope at a magnification of 100-fold.

Immunohistochemistry and senescence assay. Freshly harvested tissues were embedded with OCT and frozen in dry ice. Briefly, 10-μm-thick cryosections of liver were fixed in acetone and incubated with anti-CD3 antibody (BD Pharmingen) and alkaline phosphatase-conjugated secondary antibody. The sections were developed with alkaline phosphatase blue substrate using alkaline phosphatase substrate kit III (Vector). Staining with hematoxylin and eosin was also

performed on 10-μm-thick thymus cryosections. Senescence-associated (SA) β-galactosidase staining was performed in thymus cryosections using a senescence β-galactosidase staining kit (Cell Signaling Technology).

Retroviral infection of purified CD4 T cells. Mouse $CD4^+$ T cells were isolated with a $CD4^+$ T-cell isolation kit (Miltenyi). $CD4^+$ T cells were activated with plate-bound anti-CD3 (1 μg/ml) and anti-CD28 (1 μg/ml) antibodies. Cells were then infected with a murine stem cell virus-based retrovirus coexpressing human CD8 and stabilized mouse β-catenin. Forty-eight hours after infection, human $CD8^+$ cells were sorted, and mRNA was extracted.

Detection of TCRβ rearrangement by PCR. PCR-based analysis of TCRβ-chain rearrangement was done as previously described (62). DJ rearrangement was detected using a 5′ primer upstream of the D2.1 coding region and a 3′ primer downstream of the J2.6 coding region. Vα-Jα rearrangements were detected using the same PCR strategy by using a pool of 5′ primers specific for three Vα elements and 3′ primers specific for individual Jα segments. The pictures are inverted images of ethidium bromide gels. Primer sequences are available upon request.

Cytogenetics and statistical analysis. Metaphase preparations were made from either the total thymocytes or bead-fractionated DN thymocytes with Colcemid (100 ng/ml; Gibco BRL) for 0.5 to 2 h and 0.3% KCl at 37°C for 20 min, fixed in methanol-acetic acid (3:1), and dropped onto slides in a Thermotron CDS-5 apparatus (Thermotron Industries). Chromosome-painting probes were prepared from degenarate oligonucleotide primer-PCR-amplified flow-sorted mouse chromosomes, and spectral karyotyping (SKY) hybridization and detection was performed according to standard protocols (33). The chromosomes were counterstained with DAPI. Microscopy was performed using a Leica DM-RXA microscope (Leica) with appropriate filter cubes (Chroma Technology Corp.). Fluorescence in situ hybridization images were acquired using a Photometrics charge-coupled-device camera and CW4000 imaging software (Leica). SKY images were acquired and analyzed as previously described (33). Both structural and numerical chromosome aberrations were enumerated for those samples analyzed by SKY (see Table S2 in the supplemental material for more details).

RESULTS

Expression of oncogenic β-catenin induces growth arrest and OIS in DN thymocytes in vivo. To study the role of β-catenin in T-cell development and oncogenesis, we expressed an oncogenic form of the human β-catenin gene specifically in thymocytes and T cells using the Lck promoter. The expression of the transgenic human β-catenin mRNA was undetectable in DN2 cells and was detected at low levels in DN3 and at higher levels in DN4 cells (Fig. 1A, left). Western blot analysis showed the expression of the transgenic β-catenin protein in DN4 but not in the precursor DN3 population (Fig. 1A, right). Beyond the DN4 stage, transgenic β-catenin is expressed in all subsequent thymocyte subsets at levels that mirror endogenous protein levels (40, 67). While each thymocyte subset, as assessed by CD4 and CD8 surface staining, was present in CAT-Tg mice, there was an age-dependent decrease in thymic cellularity compared to control C57BL/6 mice (see Fig. S1 in the supplemental material) (66). Thus, the expression of oncogenic β-catenin in DN4 cells and all subsequent stages of thymocytes resulted in thymic involution.

To determine the reason for the decreased levels of thymocytes, we assessed proliferation using in vivo BrdU incorporation analysis. CAT-Tg DN4 thymocytes incorporated significantly less BrdU than those of control mice, indicating impaired proliferation (Fig. 1B). Molecular analysis showed that *cyclin D3*, the major cyclin known to regulate the proliferation of DN thymocytes (58), was not affected (see Fig. S2a in the supplemental material). The cyclin-dependent kinase (cdk) inhibitors *p19*, *p21*, and *p27* were also not appreciably affected by oncogenic β-catenin (Fig. 1C; see Fig. S2a in the supplemental material). However, the expression of *p15* and *p16*, inhibitors of cdk4/6, essential for the G_1 stage of the cell cycle, was significantly induced (Fig. 1C; see Fig. S2a in the supplemental material). To demonstrate that this was a consequence of β-catenin stabilization, we expressed stabilized β-catenin in purified mature $CD4^+$ T cells using retrovirus infection and noted increased levels of *p15* and *p16* expression (see Fig. S2b in the supplemental material). We conclude that β-catenin expression induces the expression of *p15* and *p16* in thymocytes and T cells.

The expression of p15 and p16 is associated with cellular senescence (2, 6, 36). We therefore assayed the expression of other SA genes, *Dec1* (6), cadherin 16 (*cdh16*), and cathepsin F (*ctsf*) (3, 57), in sorted CAT-Tg DN4 thymocytes. *Ctsf* and *cdh16* were dramatically induced, while *Dec1* was modestly upregulated in DN4 thymocytes from CAT-Tg mice (Fig. 1D). Another marker of cellular senescence is SA β-galactosidase activity (11). SA β-galactosidase activity was also recently shown to be associated with human premalignant cells, suggesting that senescence may precede tumor formation (2, 5, 6, 38). Consistent with the upregulation of SA genes, cryosections of the CAT-Tg thymus stained for SA β-galactosidase activity showed islands of blue staining (Fig. 1E, right). Similar staining was not observed in age-matched C57BL/6 mouse thymuses (Fig. 1E, left). These data demonstrate that the expression of oncogenic β-catenin results in OIS in developing CAT-Tg thymocytes in vivo.

Expression of oncogenic β-catenin results in DNA damage and apoptosis in DN thymocytes. Recently, OIS was linked to DNA damage (1, 10, 35). Indeed, γH2AX foci, as reporters of DNA damage and DSBs (49), were observed in CAT-Tg DN but not C57BL/6 DN thymocytes (Fig. 2A). A higher-resolution analysis showed discrete foci, indicating that γH2AX staining resulted from DNA damage (Fig. 2B). CAT-Tg DN but not CAT-Tg DP thymocytes showed a dramatic increase in γH2AX foci (Fig. 2A, left). DN and DP thymocytes from C57BL/6 mice were used as negative controls (Fig. 2A, right). Irradiated total C57BL/6 thymocytes were used as positive controls (data not shown). Quantification showed that nearly half of the DN cells in CAT-Tg mice were γH2AX positive (Fig. 2A; see Fig. S3 in the supplemental material). γH2AX foci recruit DSB repair proteins and dissolve when DNA repair is completed; thus, γH2AX foci in CAT-Tg DN thymocytes indicated sustained DNA damage. As CAT-Tg DP thymocytes do not show γH2AX foci (Fig. 2A), we conclude that only those CAT-Tg DN thymocytes that adequately repair their DNA or never encountered DNA damage progress to the DP stage. We suggest the this may be one reason for the lowered thymic cellularity in CAT-Tg mice.

We next measured apoptosis levels to determine if genotoxic stress (DNA damage) was inducing cell death. CAT-Tg DN4 thymocytes consistently demonstrated higher levels of apoptosis than C57BL/6 DN4 thymocytes (Fig. 2C). We believe that CAT-Tg DP thymocytes do not experience enhanced apoptosis because the expression of endogenous and transgenic β-catenin is diminished in DP thymocytes (40, 67; data not shown). Oncogenic β-catenin has been shown to activate p53 function in several tissues and cell lines (7), and p53 is known to regulate senescence, genotoxic stress, and apoptosis. We therefore assayed for the expression of several p53 signaling-associated genes in CAT-Tg DN4 thymocytes. Four of six genes, *Ddit4*,

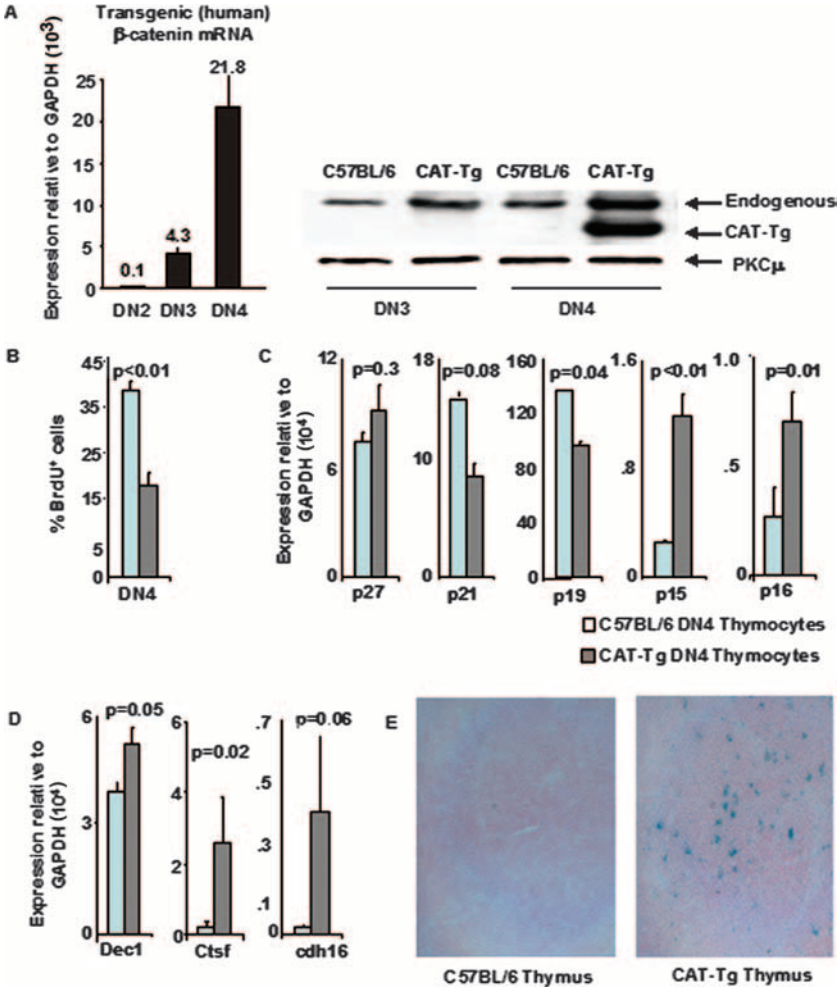

FIG. 1. Expression of stabilized β-catenin in thymocytes causes growth arrest and cellular senescence. (A) Abundance of human (transgenic) β-catenin mRNA relative to GAPDH in sorted CAT-Tg DN2, DN3, and DN4 cells analyzed by real-time PCR ($n = 3$). Shown is Western blot analysis of endogenous murine (upper bands) and transgenic human (lower bands) β-catenin protein (representative of data from five mice). (B) BrdU incorporation in electronically gated DN4 thymocytes from C57BL/6 and CAT-Tg mice. The graph shows average data from more than three mice for each genotype in one experiment and is representative of three experiments. (C) Real-time RT-PCR analysis of the expression of cell cycle regulators in sorted DN4 thymocytes from C57BL/6 ($n = 3$) and CAT-Tg ($n = 3$) mice. (D) Real-time PCR analysis of SA genes in sorted DN4 thymocytes from C57BL/6 and CAT-Tg mice ($n = 3$). (D) SA β-galactosidase activity in thymic cryosections from C57BL/6 and CAT-Tg mice (representative of $n = 4$).

PUMA, *Gadd45*β, and *Gadd45*γ, showed significant induction, whereas the expression of *Gadd45*α and *Sesn1* remained unchanged (Fig. 2D). These data demonstrate that oncogenic β-catenin expression in DN4 thymocytes triggers a stress response leading to the activation of p53-mediated signaling pathways.

β-Catenin induces p53-independent DNA damage and OIS in thymocytes. To test the functional significance of β-catenin-induced p53 function in thymocytes, we bred CAT-Tg mice to p53-deficient mice to generate $p53^{-/-}$ CAT-Tg mice. First, we analyzed the number of thymocytes in $p53^{-/-}$ CAT-Tg mice. Mice up to 35 days of age showed greater than 100×10^6 cells, which is normal. Thymocyte numbers declined at between 36 and 65 days of age and increased after 66 days (Fig. 3A). The decline in thymocyte numbers in $p53^{-/-}$ CAT-Tg mice aged 36 to 65 days could be attributed to DNA damage, OIS, and growth arrest (Fig. 3B, C, and E). $p53^{-/-}$ CAT-Tg DN thymocytes showed DNA damage, while $p53^{-/-}$ DN thymocytes did not (Fig. 3B). Also, tissue sections of $p53^{-/-}$ CAT-Tg thymus showed SA β-galactosidase activity (Fig. 3C). However, the increased cell death observed in CAT-Tg DN4 thymocytes compared to C57BL/6 DN4 thymocytes was abrogated in $p53^{-/-}$ CAT-Tg DN4 thymocytes (Fig. 3D). These data demonstrate that β-catenin-induced DNA damage, OIS, and growth arrest are p53 independent, while apoptosis is p53 dependent. The subpopulation of the growth-arrested $p53^{-/-}$ CAT-Tg thymocytes that could not undergo p53-dependent apoptosis began proliferating, ultimately resulting in thymic lymphoma. To determine the molecular basis for the proliferation, we studied the difference between $p53^{-/-}$ CAT-Tg DN cells that efficiently incorporate BrdU (post-66 days) and those that did not (36 to 65 days) (Fig. 3E). The increased proliferation after 66 days could be attributed to the decreased expression of the cell cycle inhibitor *p21* in a subset of DN cells

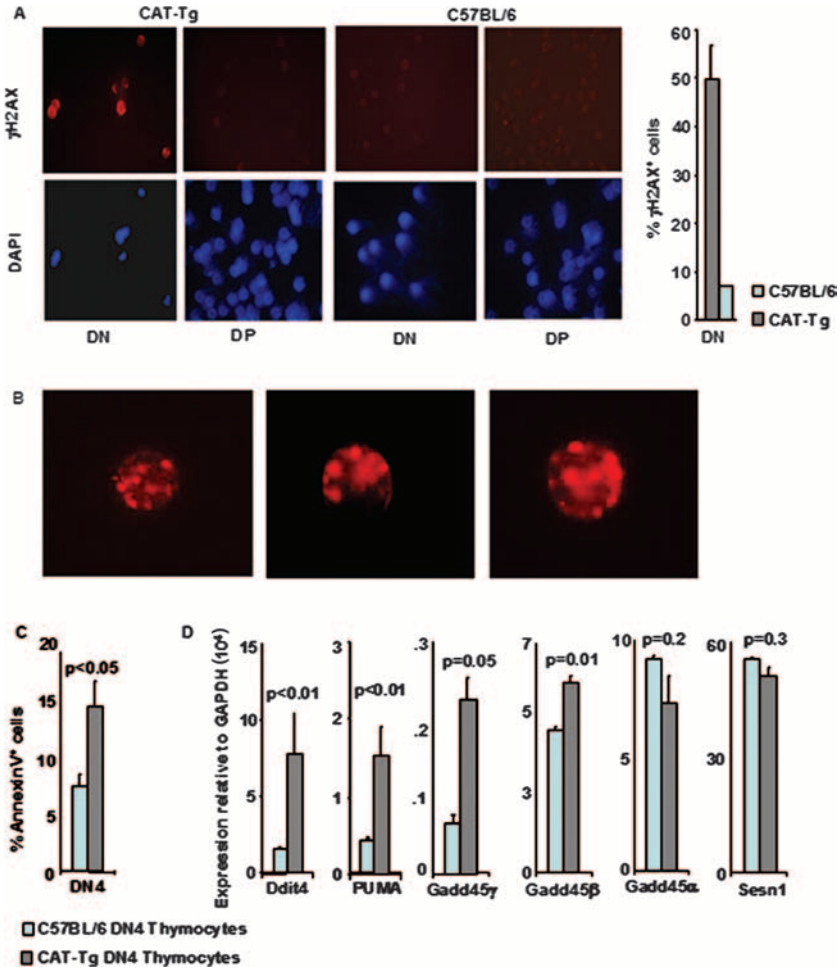

FIG. 2. Enhanced DNA damage and p53-dependent apoptosis in CAT-Tg mice. (A) Immunofluorescence staining of phosphorylated histone γH2AX in fixed DN (eight CAT-Tg and C57BL/6 mice) and DP (two CAT-Tg and two C57BL/6 mice) thymocytes. The bar graph shows the percentage of γH2AX-positive cells in C57BL/6 DN and CAT-Tg DN thymocytes (see Fig. S3 in the supplemental material). (B) Three examples of γH2AX foci in CAT-Tg DN thymocytes shown at a higher magnification. (C) Annexin V staining of DN4 thymocytes (electronically gated) from C57BL/6 and CAT-Tg mice. The numbers in the graph are an average of data from more than three mice for each genotype in one experiment that is representative of six experiments. (D) Real-time RT-PCR analysis of the expression of p53 pathway-associated genes in sorted DN4 thymocytes from CAT-Tg ($n = 3$) and C57BL/6 ($n = 3$) mice.

(Fig. 3F; see Fig. S5 in the supplemental material). In the $p53^{-/-}$ CAT-Tg DN population, senescent cells, cells expressing *p15* and *p16*, and growth-arrested cells expressing several other cell cycle inhibitors were also noted (Fig. 3F). We conclude that p53 expression can prevent oncogenic β-catenin-induced thymic lymphoma.

Aggressive thymic lymphomas develop at an earlier age in $p53^{-/-}$ CAT-Tg mice. Previous studies suggested that the abrogation of p53-induced apoptosis may be sufficient for lymphoma development (27). Kaplan-Meier analysis of a cohort of 14 $p53^{-/-}$ CAT-Tg mice showed that the median time to death of $p53^{-/-}$ CAT-Tg mice (73 days; 7 of 14 mice died by day 73, and the rest died by day 91) was dramatically decreased compared to that of CAT-Tg (>300 days) or p53-deficient (165 days) mice (Fig. 4A, right) (32, 41). In the colony of $p53^{-/-}$ CAT-Tg mice over a 2-year period, only three mice lived beyond 91 days for reasons not understood. These mice were sacrificed on days 92, 99, and 109 postbirth when they were terminally ill and showed characteristic thymic lymphomas. The data in Fig. 4B show that 12 of 13 mice dissected between 66 and 91 days of age exhibited thymic lymphoma, while none of their $p53^{+/-}$ CAT-Tg or $p53^{-/-}$ littermates did. These data demonstrate that the decreased life span in $p53^{-/-}$ CAT-Tg mice was the result of an accelerated initial onset of thymic lymphoma and suggest a synergistic interaction between oncogenic β-catenin and a loss of p53 function.

$p53^{-/-}$ CAT-Tg mice that died early invariably displayed enlarged thymus, spleen, and lymph nodes (Fig. 4C) accompanied by lymphoblastic T-cell infiltration into nonlymphoid organs such as liver (Fig. 4D). Histological examination of lymphoma-bearing thymuses from $p53^{-/-}$ CAT-Tg mice revealed enlarged thymocytes and a loss of thymic architecture (data not shown). Infiltration of DN lymphoma cells into nonlymphoid tissues such as the liver (Fig. 4D) and into the spleen and lymph nodes (Fig. 4E to G) demonstrated the metastatic potential of the DN lymphoma in $p53^{-/-}$ CAT-Tg mice.

Progression of lymphoma development in $p53^{-/-}$ CAT-Tg mice. Thymocyte numbers increased after 66 days of age in

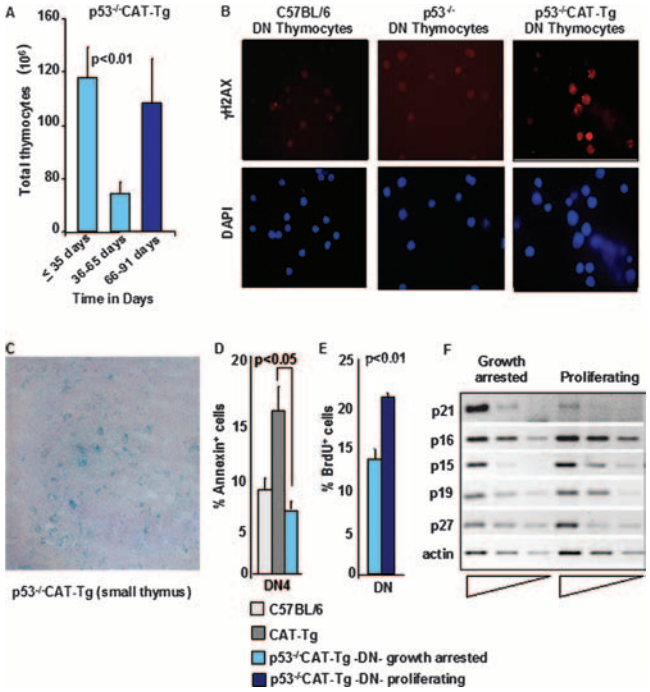

FIG. 3. Expression of stabilized β-catenin induces p53-independent DNA damage and OIS and p53-dependent apoptosis in thymocytes. (A) Total number of thymocytes in $p53^{-/-}$ CAT-Tg mice at different ages. The first two bars (light blue) represent the initial decrease in thymic cellularity in young mice, and the right bar (dark blue) indicates regained thymic cellularity after 66 days of age. (B) Immunofluorescence staining of γH2AX in fixed DN cells from C57BL/6, $p53^{-/-}$, and $p53^{-/-}$ CAT-Tg mice. (C) SA β-galactosidase expression in cryosections from a 50-day-old lymphoma-free $p53^{-/-}$ CAT-Tg mouse with a small thymus. (D) Annexin V staining of electronically gated DN4 thymocytes from C57BL/6, CAT-Tg, and lymphoma-free $p53^{-/-}$ CAT-Tg mice (≤65 days old). The data are averages of data from more than three mice for each genotype in one experiment, which is representative of four experiments. (E) BrdU incorporation in electronically gated DN thymocytes from young and lymphoma-free $p53^{-/-}$ CAT-Tg mice (growth arrested) and relatively old lymphoma-bearing $p53^{-/-}$ CAT-Tg mice (proliferating). The graph shows the average of data from more than two mice for each genotype in one experiment and is representative of two experiments. (F) RT-PCR analysis of the expression of cell cycle regulators in sorted DN thymocytes from young lymphoma-free $p53^{-/-}$ CAT-Tg mice (growth arrested) ($n = 3$) and old lymphoma-bearing $p53^{-/-}$ CAT-Tg mice (proliferating) ($n = 3$).

$p53^{-/-}$ CAT-Tg mice (Fig. 3A), resulting in thymic lymphoma. We characterized the development and progression of $p53^{-/-}$ CAT-Tg lymphoma. Flow cytometry profiles for thymocytes from CAT-Tg and C57BL/6 control mice were similar with respect to both their size distributions and percentages of DN, DP, CD4SP, and CD8SP populations (Fig. 5A and B). Interestingly, in a time-dependent manner, DN thymocytes accumulated in $p53^{-/-}$ CAT-Tg mice at the cost of DP and to some extent SP thymocytes (Fig. 5C). As demonstrated in Fig. 3A, thymocyte numbers declined, suggesting that the accumulation of DN thymocytes was at the cost of DP and SP thymocytes. Finally, after about 66 days of age, the number of thymocytes in $p53^{-/-}$ CAT-Tg mice increased, and the major population of cells was c-kit$^-$ CD25$^-$ (see Fig. S4 in the supplemental material) as well as CD4$^-$ CD8$^-$ and expressed intermediate levels of the TCRβ chain on the cell surface (Fig. 5C). This phenotype corresponds to the aberrant thymocyte population that results in β-catenin-dependent thymic lymphoma.

Interestingly, in a cohort of 30 $p53^{+/-}$ CAT-Tg mice, 15 died or were terminally ill with thymic lymphomas by the age of 160 days, and all died by day 241 (Fig. 4A). In contrast, $p53^{+/-}$ mice lived beyond 270 days (32, 41). The lymphomas in the $p53^{+/-}$ CAT-Tg mice were phenotypically identical to those found in $p53^{-/-}$ CAT-Tg mice (Fig. 5D). The accelerated death of $p53^{+/-}$ CAT-Tg mice and the phenotype of the lymphoma suggested a loss of heterozygosity at the p53 locus. Using a PCR-based assay (2), we documented the loss of the wild-type allele of p53 in three independent $p53^{+/-}$ CAT-Tg thymic lymphomas, a representative of which is shown in Fig. 5E. Therefore, we conclude that a complete loss of p53 expression in thymocytes is essential for β-catenin to exert its oncogenic effect.

$p53^{-/-}$ CAT-Tg DN lymphomas are immature and molecularly distinct from DP lymphomas that develop in $p53^{-/-}$ mice. Sixty to eighty percent of the spontaneous malignancies in p53-deficient mice are thymic lymphomas (32, 41). To unambiguously demonstrate that the β-catenin-dependent thymic lymphomas in $p53^{-/-}$ CAT-Tg mice were distinct from $p53^{-/-}$ lymphomas, we evaluated their phenotypes and molecular characteristics. Thymocytes from both $p53^{-/-}$ and $p53^{-/-}$ CAT-Tg tumor burden thymuses showed a preponderance of large cells (Fig. 5C and D and 6A). The phenotypes of all the cells in the thymus indicated that the $p53^{-/-}$ thymic lymphoma consisted of ~46% DP and ~34% CD8SP cells (Fig. 6A) (21, 32). Indeed, the DN population in $p53^{-/-}$ mice was normal and comparable to the DN population from C57BL/6 mice with respect to the distribution of DN1 to DN4 as judged by c-kit and CD25 staining (see Fig. S4 in the supplemental material) and cell surface TCRβ staining (Fig. 6A). In gross contrast, in the $p53^{-/-}$ CAT-Tg or $p53^{+/-}$ CAT-Tg thymuses, a DN lymphoma population expressing intermediate levels of TCRβ/CD3 accounted for 86% of thymocytes, respectively (Fig. 5C and D). Thus, the β-catenin-induced lymphomas in $p53^{-/-}$ CAT-Tg mice are phenotypically distinct from those that develop in $p53^{-/-}$ mice at an older age. Furthermore, *Notch1* or c-*Myc* genes have been implicated in T-cell lymphomas (46, 60, 64). Interestingly, neither Notch signaling nor c-Myc upregulation was noted in $p53^{-/-}$ CAT-Tg thymic DN lymphomas (Fig. 6B).

The DN lymphoma cells in $p53^{-/-}$ CAT-Tg mice express intermediate levels of TCRβ on their cell surfaces (Fig. 5C and D). To eliminate the possibility that these DN cells were mature thymocytes that had lost the expression of CD4 and CD8, we assayed for the expression of several TCRα proteins. Cell surface TCRα expression was not detected in DN thymocytes (Fig. 6C, top) but was detectable on DP and SP populations from C57BL/6 or $p53^{-/-}$ CAT-Tg mice (Fig. 6C, bottom). Furthermore, PCR-based analysis of DNA rearrangements at the TCRα chain locus revealed a lack of TCRα rearrangement (Fig. 6D). A similar analysis of the TCRβ chain locus showed that the thymic lymphomas in $p53^{-/-}$ CAT-Tg thymuses were oligoclonal (Fig. 6E), thereby demonstrating that the oligoclonal DN lymphoma cells in $p53^{-/-}$ CAT-Tg mice are actually transformed pre-DP cells of immature thymocyte origin.

SKY of DN $p53^{-/-}$ CAT-Tg thymic lymphoma cells re-

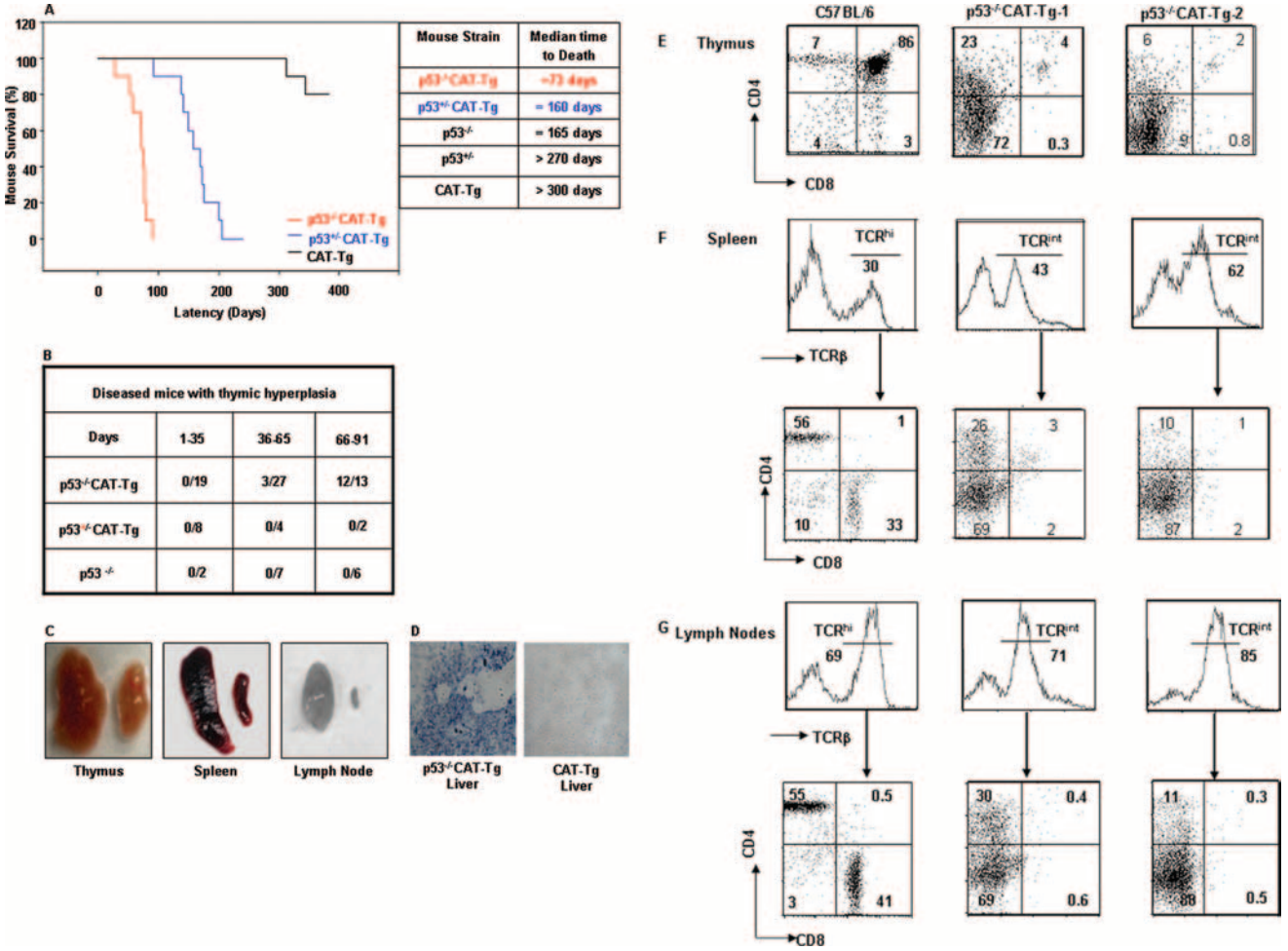

FIG. 4. Stabilized β-catenin in a p53-deficient genetic background causes thymic lymphoma and death of the mice at an early age. (A) Kaplan-Meier plot showing time-to-death latencies in CAT-Tg ($n = 10$), $p53^{-/-}$ CAT-Tg ($n = 14$), and $p53^{+/-}$ CAT-Tg ($n = 30$) mice. Kaplan-Meier plots for $p53^{-/-}$ and $p53^{+/-}$ mice were reported previously (41). The insert indicates the median time to death of mice with various genotypes. (B) Numbers of mice with thymic hyperplasia in a cohort of $p53^{-/-}$ CAT-Tg, $p53^{+/-}$ CAT-Tg, and $p53^{-/-}$ mice. (C) Thymus, spleen, and lymph nodes from diseased $p53^{-/-}$ CAT-Tg mice (70 days old) (left) and C57BL/6 mice (56 days old) (right). (D) Immunohistochemical analysis of CD3ε expression (blue) in cryosections of livers from a diseased $p53^{-/-}$ CAT-Tg mouse (84 days old) and a CAT-Tg mouse (84 days old) at 20-fold magnification. (E to G) Thymocytes (E), splenocytes (F), and lymph node cells (G) from C57BL/6 mice (left) and two $p53^{-/-}$ CAT-Tg mice ($p53^{-/-}$ CAT-Tg-1 mice [79 days old] and $p53^{-/-}$ CAT-Tg-2 mice [84 days old] [two right panels]) were stained with antibodies to the TCRβ chain, CD4, and CD8 and analyzed by flow cytometry. Histogram of TCRβ chain expression and dot plots for CD4 and CD8 expression on gated $TCR\beta^{int/hi}$ splenocytes and lymph node cells are shown.

vealed chromosome alterations (Fig. 6F and G; see Tables S1 and S2 in the supplemental material). The structural aberrations included clonal and nonclonal chromosome rearrangements of various configurations, including chromosomes with multiple centromeres, chromosome and chromatid breaks, chromosome deletions, and centromere and acentric fragments (Fig. 6F; see Table S1 in the supplemental material). In addition, the numbers of chromosomes were increased in cells from all the samples analyzed (see Fig. 6G for examples), and this substantial polyploidy in the $p53^{-/-}$ CAT-Tg lymphomas was reflected in an increase in chromosome instability or missegregation errors ($P = 0.028$) (see Table S1 in the supplemental material). Importantly, these distinctive chromosomal alterations were not observed in the control C57BL/6 thymocytes and are distinct from those reported in $p53^{-/-}$ lymphomas (21, 32).

Whereas many chromosomes were affected, the majority of cells from all five $p53^{-/-}$ CAT-Tg lymphomas showed a loss of chromosome 13, and three of the five $p53^{-/-}$CAT-Tg lymphomas showed a gain of chromosome 17 (see Table S2 in the supplemental material). In contrast, in $p53^{-/-}$ lymphoma cells, a frequent gain of chromosome 1, 4, 5, or 15 has been reported (32). Moreover, the pattern of chromosome translocations harbored by $p53^{-/-}$ CAT-Tg lymphoma cells was random and showed little similarity to that of $p53^{-/-}$ lymphoma cells (32). These $p53^{-/-}$ CAT-Tg lymphomas were also distinct from the lymphomas observed in NHEJ $p53^{-/-}$ mice and $ATM^{-/-}$ thymic lymphomas, which are characterized by chromosome translocations involving the immunoglobulin or TCR locus, respectively (8, 9, 51, 68). These abnormalities therefore define unique features of cells transformed by oncogenic β-catenin in the absence of p53. Of note, significant genomic instability was

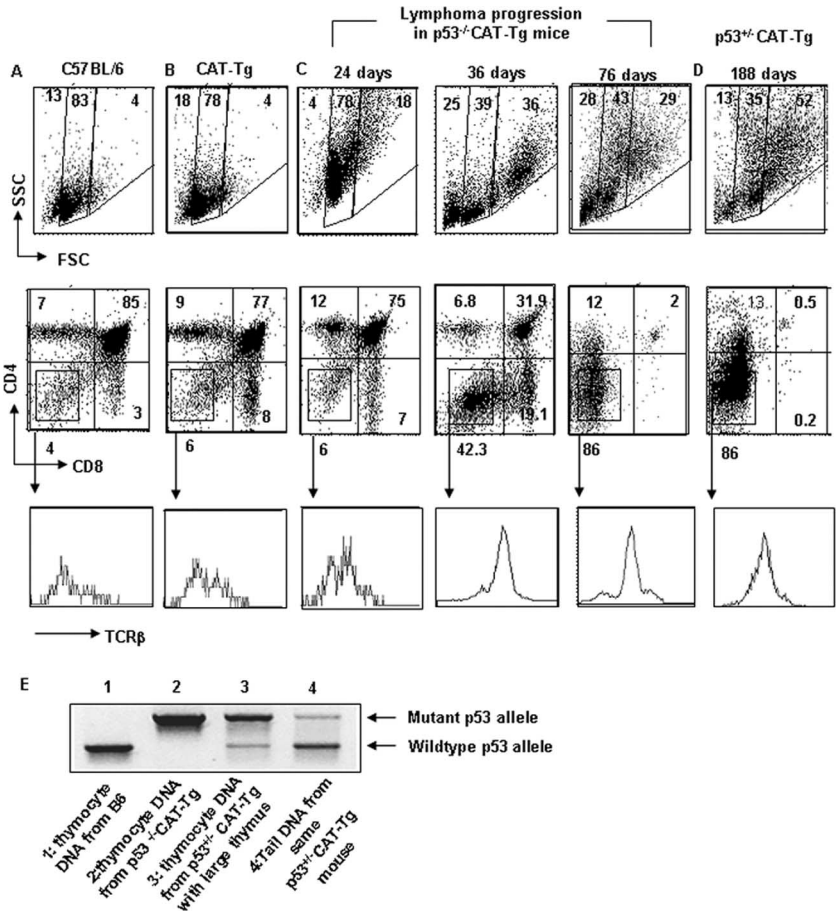

FIG. 5. Lymphoma progression in $p53^{-/-}$ CAT-Tg mice and loss of p53 function are essential for the formation of β-catenin-triggered DN thymic lymphoma. (A to D) Representative fluorescence-activated cell sorter profiles showing forward scatter (FSC) and side scatter (SSC) (top) and cell surface staining of CD4 and CD8 (middle) and TCRβ (bottom) in electronically gated $CD4^-$ $CD8^-$ DN cells of total thymocytes from C57BL/6 mice ($n > 10$) (A), CAT-Tg mice ($n > 10$) (B), $p53^{-/-}$ CAT-Tg mice ($n > 4$) at different ages as indicated (C), and $p53^{+/-}$ CAT-Tg mice bearing thymic lymphoma ($n > 5$). (E) Allele-specific p53 genomic PCR detects normal wild-type and mutant p53 allele (tail) tissues but largely the mutant allele in the thymic lymphoma (representative of three independent thymic lymphomas).

detected in DN thymocytes purified from both CAT-Tg and $p53^{-/-}$ CAT-Tg mice, indicating that the initial chromosomal instability was triggered by the oncogenic expression of β-catenin (see Table S1 in the supplemental material). Thus, it appears that the expression of oncogenic β-catenin initiates chromosomal instability in developing thymocytes that is manifest in the absence of p53 expression. Taken in total, these data demonstrate the unique nature of β-catenin-induced thymic lymphomas and their distinction with regard to both their phenotype and molecular etiology compared to those of tumors that develop in p53-deficient mice.

DISCUSSION

In this report, we demonstrate that oncogenic β-catenin induces p53-independent DNA damage and OIS in vivo in developing thymocytes, followed by p53-dependent apoptosis of damaged cells. This sequence of events prevents the development of β-catenin-dependent thymic lymphoma in immature thymocytes. While it has been shown in cell lines that DNA damage triggers OIS, our studies show for the first time that enhanced DNA damage signaling may be linked to OIS in developing animal tissues. Notably, these studies show that DNA damage and OIS are p53 independent, while apoptosis is p53 dependent. Because β-catenin has been demonstrated to be essential for β selection (15, 45, 65), these studies propose for the first time that in instances when an oncogene is utilized for signal transduction during normal development, a number of mechanisms that prevent oncogenesis are instituted.

It is well established that the oncogenic expression of β-catenin leads to tumorigenesis in several tissues, including colon, breast, and skin (13, 23, 34, 44, 48). It was therefore surprising that CAT-Tg mice showed decreased thymic cellularity and accelerated thymic involution instead of thymic lymphoma (66). It is further intriguing that human β-catenin-dependent T-cell lymphomas have also not been documented to date. Studies reported here provide a molecular reason for these observations. The initial response of DN thymocytes to oncogenic β-catenin was sustained DNA damage and p53-independent OIS. While it was unclear if DNA-damaged cells went on to senescence, it was clear that both DNA damage and OIS were p53 independent. Damaged DN thymocytes were elimi-

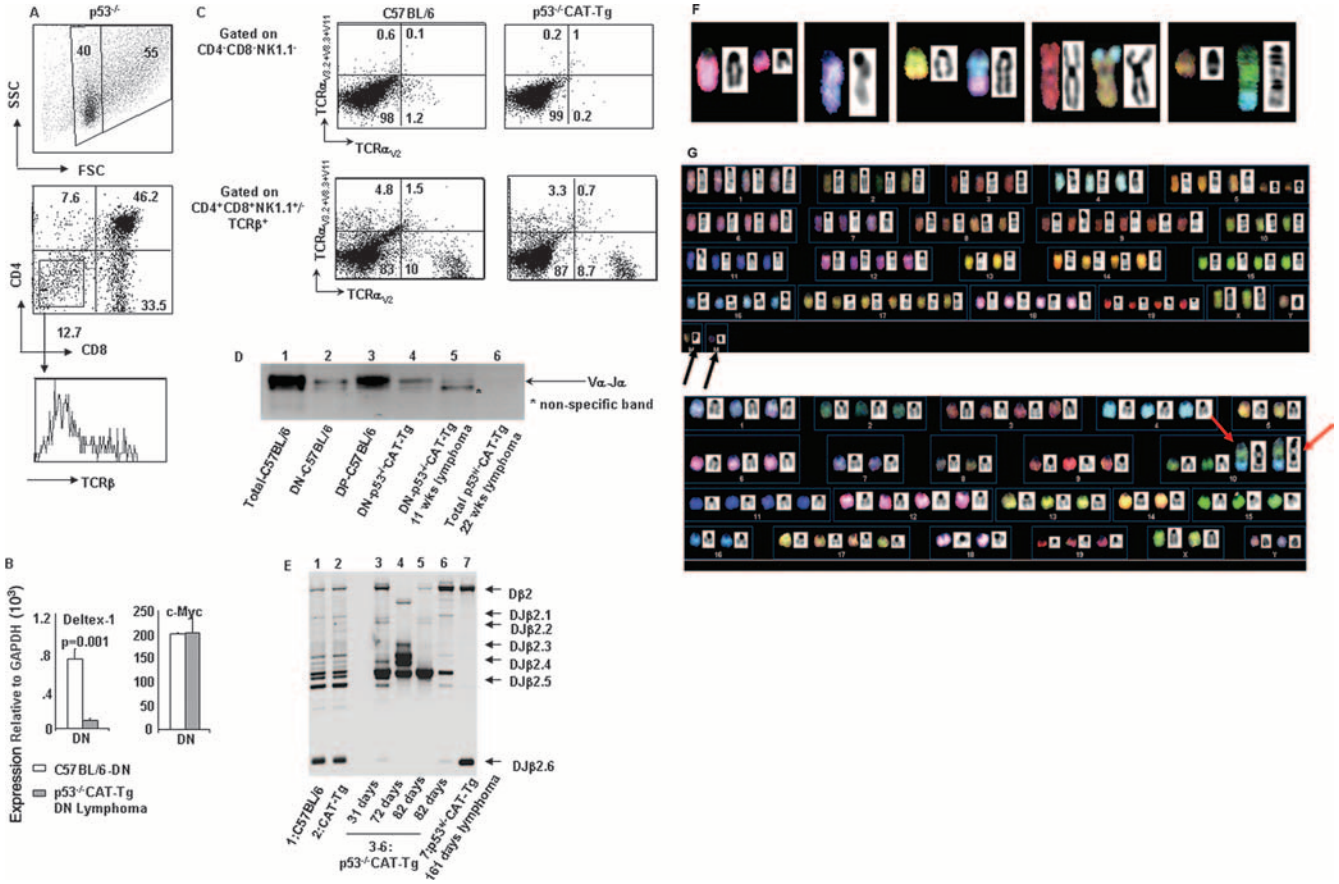

FIG. 6. $p53^{-/-}$ CAT-Tg DN lymphomas are immature pre-DP cells and are distinct from $p53^{-/-}$ DP/SP lymphomas. (A) Representative fluorescence-activated cell sorter profiles showing forward scatter (FSC) and side scatter (SSC) (top) and cell surface staining of CD4, CD8 (middle), and TCRβ (bottom) on electronically gated $CD4^-$ $CD8^-$ DN cells of total thymocytes from a thymic lymphoma-bearing 91-day-old $p53^{-/-}$ mouse. (B) Abundance of Deltex-1 and c-Myc mRNA relative to GAPDH in DN thymocytes from C56BL/6 and lymphoma-bearing $p53^{-/-}$ CAT-Tg mice analyzed by real-time PCR. (C) Total thymocytes from C57BL/6 and lymphoma-bearing $p53^{-/-}$CAT-Tg mice were stained with a group of TCRα antibodies. (Top) Surface expression of TCRα on thymocytes electronically gated to exclude DP, SP, and NK cells. (Bottom) Surface expression of TCRα on electronically gated DP and SP thymocytes. (D) PCR analysis of rearranged $TCR\alpha V_{5H+F3+2C}$-J_{2T11} gene segments using the same amount of genomic DNA purified from thymocytes. (E) PCR analysis of rearranged TCRβD2-Jβ2 gene segments using same amount of genomic DNA purified from total thymocytes. (F) Chromosome structural aberrations in $p53^{-/-}$ CAT-Tg lymphomas. From left to right, a normal chromosome 6 (left), a deleted chromosome 6 (right), a chromatid break on chromosome 11, and chromosome translocations illustrated by T(10;17) (left) and T(4;6) (right) are shown; centromere fusions were sometimes simple, containing material from the same chromosome, as in Rb(3.3) on the left, and sometimes more complex, as in Rb[5.T(5;4)] on the right. Polycentric chromosomes resulted from the fusion of chromosomes in a tail-to-tail orientation, as in the dicentric chromosome on the left, or in a head-to-tail orientation, as occurred multiple times in the pentacentric chromosome on the right. (G) Spectral karyotype of $p53^{-/-}$ CAT-Tg lymphomas. The top metaphase is a pseudotetraploid cell ($n = 80$) with deletions of chromosome 5, a general loss of chromosome 13, and a gain of chromosome 17. Also illustrated at the bottom left side are two chromosome fragments containing centromeres (black arrows). The bottom cell is a pseudotriploid ($n = 60$) karyotype with a complex rearrangement between chromosomes 10 and 16 containing four centromeres (red arrows).

nated by p53-dependent cell death. Together, these events prevented the development of β-catenin-induced thymic lymphoma. These data complement studies in which high levels of retrovirally expressed oncogenic β-catenin in hematopoietic tissues also failed to cause lymphomas for up to 6 months in mice (52). We propose that studies in this report have uncovered a β-catenin-dependent mechanism that identifies DNA-damaged thymocytes during the transition of DN thymocytes to the DP stage, induces p53-independent OIS, and activates p53-dependent cell death.

Recently, Guo et al. induced oncogenic β-catenin in mice by deleting floxed exon 3 before β selection using Lck-Cre and after β selection using CD4-Cre (20). In CD4-Cre-$Ctnnb^{\Delta ex3}$ mice, the thymic lymphomas formed were DP in phenotype and resulted from the induction of the β-catenin target gene, c-Myc. Indeed, Guo et al. demonstrated that the thymic lymphomas were c-Myc dependent and were abrogated if c-Myc was deleted. In CAT-Tg mice, the transgenic protein is expressed in DN4 cells prior to β selection, increasing the amount of β-catenin to two- to fourfold above that induced during β selection (Fig. 1A). In this model, β-catenin expression results in DNA damage, OIS, and growth arrest in developing thymocytes, followed by the p53-dependent death of damaged cells, preventing β-catenin-dependent thymic lymphomas. The level of stabilized oncogenic β-catenin resulting from an exon 3 deletion is much higher than the two- to

threefold induction during normal signaling events. Despite high levels of oncogenic β-catenin expression in DN thymocytes, the incidence of thymic lymphoma was significantly lower in Lck-Cre-Ctnnb$^{\Delta ex3}$ mice than in CD4-Cre-Ctnnb$^{\Delta ex3}$ mice. In our model, the abrogation of p53-dependent apoptosis leads to thymic lymphoma. Guo et al. did not address the role of p53 in the few incidences of thymic lymphomas in the Lck-Cre-Ctnnb$^{\Delta ex3}$ mice. Together, these data suggest that an increased expression of β-catenin prior to β selection does not lead to thymic lymphoma.

β-Catenin has been demonstrated to be essential for β selection (15, 45, 65). However, during normal thymocyte maturation, after β selection and prior to the transition to the DP stage, β-catenin expression is significantly downregulated (67). We suggest that DP thymocytes do not have molecular mechanisms to downregulate β-catenin, resulting in the induction of target gene c-Myc-dependent DP lymphomas (20). Thus, this report provides a mechanism for the observation that the induction of oncogenic β-catenin prior to β selection results in significantly fewer incidences of thymic lymphoma. We suggest that this is because when an oncogene is utilized as a normal part of signal transduction, built-in molecular mechanisms provide protection from transformation.

Thymic lymphomas have been documented in p53$^{-/-}$, p53$^{-/-}$ RAG$^{-/-}$, and p53$^{-/-}$ CD3γ$^{-/-}$mice. One striking feature of these thymic lymphomas is that tumor cells have a DP or SP phenotype (21, 32, 41). Because a p53 deficiency permits the maturation of normal DN thymocytes to the DP stage, it remains unresolved whether transformation took place at the DN stage, followed by further differentiation to the DP and SP stages, or if it occurred subsequent to maturation in these mice. Lymphomas in p53$^{-/-}$ CAT-Tg mice, however, were largely immature DN cells, because DNA-damaged cells were prevented from progression to the DP stage. Thus, we speculate that a β-catenin-dependent mechanism regulates the transition of normal DN cells to the DP stage of differentiation.

Model for β-catenin–p53 interactions that occur during normal thymocyte development. We suggest a model in which β-catenin induced during β selection, as an essential aspect of signal transduction during thymocyte development, must be downregulated after β selection. In the event that downregulation is prevented, thymic lymphoma would ensue; therefore, p53-independent and p53-dependent pathways have been instituted to provide protection from thymic lymphomas. The sequence of events appears to be β-catenin signal-induced growth arrest, OIS, and p53 function, which is followed by p53-dependent apoptosis of developing thymocytes that harbor DNA damage from recombination and/or replication events. In CAT-Tg mice, DN thymocytes expressing transgenic β-catenin show enhanced DSBs in growth-arrested cells and/or cells with OIS, perhaps because β-catenin expression provides survival signals. However, p53 function is also induced, and these cells die in a p53-dependent manner, with only cells with undamaged DNA proceeding to the DP stage. One consequence is reduced thymic cellularity. In p53$^{-/-}$ CAT-Tg mice, DN cells with DNA damage, growth arrest, and OIS are found, but p53-dependent apoptosis is abrogated. A fraction of growth-arrested DNA-damaged cells lose the p21-dependent cell cycle checkpoint, proliferate, and cause the observed thymic hyperplasia and lymphoma. In conclusion, this report provides evidence that p53-independent β-catenin-induced OIS and p53-dependent apoptosis serve as mechanisms by which β-catenin-induced thymic lymphoma is kept in check when β-catenin is induced as a part of signal transduction during β selection.

ACKNOWLEDGMENTS

We thank Robert Wersto, Francis J. Chrest, and Cuong Nguyen for expert cell sorting of thymocyte subpopulations; Donna Tignor, Dawn Phillips, Dawn Nines, Heather Breighner, Anna Butler, Crystal Gifford, and Ernest Dabney for maintaining animals; Shengyuan Luo and his group for genotyping animals; Susanne Golech and Dot Bertak for help in immunohistochemistry; and Linda Barenboim-Stapleton for preparation of SKY kits and chromosome-painting probes.

This research was supported by the Intramural Research Programs of the National Institute on Aging and the National Cancer Institute at the National Institutes of Health.

REFERENCES

1. **Bartkova, J., N. Rezaei, M. Liontos, P. Karakaidos, D. Kletsas, N. Issaeva, L. V. Vassiliou, E. Kolettas, K. Niforou, V. C. Zoumpourlis, M. Takaoka, H. Nakagawa, F. Tort, K. Fugger, F. Johansson, M. Sehested, C. L. Andersen, L. Dyrskjot, T. Orntoft, J. Lukas, C. Kittas, T. Helleday, T. D. Halazonetis, J. Bartek, and V. G. Gorgoulis.** 2006. Oncogene-induced senescence is part of the tumorigenesis barrier imposed by DNA damage checkpoints. Nature **444:**633–637.
2. **Braig, M., S. Lee, C. Loddenkemper, C. Rudolph, A. H. Peters, B. Schlegelberger, H. Stein, B. Dorken, T. Jenuwein, and C. A. Schmitt.** 2005. Oncogene-induced senescence as an initial barrier in lymphoma development. Nature **436:**660–665.
3. **Campisi, J.** 2001. Cellular senescence as a tumor-suppressor mechanism. Trends Cell Biol. **11:**S27–S31.
4. **Chen, H. T., A. Bhandoola, M. J. Difilippantonio, J. Zhu, M. J. Brown, X. Tai, E. P. Rogakou, T. M. Brotz, W. M. Bonner, T. Ried, and A. Nussenzweig.** 2000. Response to RAG-mediated VDJ cleavage by NBS1 and gamma-H2AX. Science **290:**1962–1965.
5. **Chen, Z., L. C. Trotman, D. Shaffer, H. K. Lin, Z. A. Dotan, M. Niki, J. A. Koutcher, H. I. Scher, T. Ludwig, W. Gerald, C. Cordon-Cardo, and P. P. Pandolfi.** 2005. Crucial role of p53-dependent cellular senescence in suppression of Pten-deficient tumorigenesis. Nature **436:**725–730.
6. **Collado, M., J. Gil, A. Efeyan, C. Guerra, A. J. Schuhmacher, M. Barradas, A. Benguria, A. Zaballos, J. M. Flores, M. Barbacid, D. Beach, and M. Serrano.** 2005. Tumour biology: senescence in premalignant tumours. Nature **436:**642.
7. **Damalas, A., S. Kahan, M. Shtutman, A. Ben-Ze'ev, and M. Oren.** 2001. Deregulated beta-catenin induces a p53- and ARF-dependent growth arrest and cooperates with Ras in transformation. EMBO J. **20:**4912–4922.
8. **Difilippantonio, M. J., S. Petersen, H. T. Chen, R. Johnson, M. Jasin, R. Kanaar, T. Ried, and A. Nussenzweig.** 2002. Evidence for replicative repair of DNA double-strand breaks leading to oncogenic translocation and gene amplification. J. Exp. Med. **196:**469–480.
9. **Difilippantonio, M. J., J. Zhu, H. T. Chen, E. Meffre, M. C. Nussenzweig, E. E. Max, T. Ried, and A. Nussenzweig.** 2000. DNA repair protein Ku80 suppresses chromosomal aberrations and malignant transformation. Nature **404:**510–514.
10. **Di Micco, R., M. Fumagalli, A. Cicalese, S. Piccinin, P. Gasparini, C. Luise, C. Schurra, M. Garre, P. G. Nuciforo, A. Bensimon, R. Maestro, P. G. Pelicci, and F. d'Adda di Fagagna.** 2006. Oncogene-induced senescence is a DNA damage response triggered by DNA hyper-replication. Nature **444:**638–642.
11. **Dimri, G. P., X. Lee, G. Basile, M. Acosta, G. Scott, C. Roskelley, E. E. Medrano, M. Linskens, I. Rubelj, O. Pereira-Smith, et al.** 1995. A biomarker that identifies senescent human cells in culture and in aging skin in vivo. Proc. Natl. Acad. Sci. USA **92:**9363–9367.
12. **Dudley, E. C., H. T. Petrie, L. M. Shah, M. J. Owen, and A. C. Hayday.** 1994. T cell receptor beta chain gene rearrangement and selection during thymocyte development in adult mice. Immunity **1:**83–93.
13. **Gat, U., R. DasGupta, L. Degenstein, and E. Fuchs.** 1998. De novo hair follicle morphogenesis and hair tumors in mice expressing a truncated beta-catenin in skin. Cell **95:**605–614.
14. **Godfrey, D. I., J. Kennedy, P. Mombaerts, S. Tonegawa, and A. Zlotnik.** 1994. Onset of TCR-beta gene rearrangement and role of TCR-beta expression during CD3−CD4−CD8− thymocyte differentiation. J. Immunol. **152:**4783–4792.
15. **Gounari, F., I. Aifantis, K. Khazaie, S. Hoeflinger, N. Harada, M. M. Taketo, and H. von Boehmer.** 2001. Somatic activation of beta-catenin bypasses pre-TCR signaling and TCR selection in thymocyte development. Nat. Immunol. **2:**863–869.
16. **Gounari, F., R. Chang, J. Cowan, Z. Guo, M. Dose, E. Gounaris, and K.**

Khazaie. 2005. Loss of adenomatous polyposis coli gene function disrupts thymic development. Nat. Immunol. **6:**800–809.
17. **Grade, M., B. M. Ghadimi, S. Varma, R. Simon, D. Wangsa, L. Barenboim-Stapleton, T. Liersch, H. Becker, T. Ried, and M. J. Difilippantonio.** 2006. Aneuploidy-dependent massive deregulation of the cellular transcriptome and apparent divergence of the Wnt/beta-catenin signaling pathway in human rectal carcinomas. Cancer Res. **66:**267–282.
18. **Gregorieff, A., and H. Clevers.** 2005. Wnt signaling in the intestinal epithelium: from endoderm to cancer. Genes Dev. **19:**877–890.
19. **Guidos, C. J., C. J. Williams, I. Grandal, G. Knowles, M. T. Huang, and J. S. Danska.** 1996. V(D)J recombination activates a p53-dependent DNA damage checkpoint in scid lymphocyte precursors. Genes Dev. **10:**2038–2054.
20. **Guo, Z., M. Dose, D. Kovalovsky, R. Chang, J. O'Neil, A. T. Look, H. von Boehmer, K. Khazaie, and F. Gounari.** 2007. Beta-catenin stabilization stalls the transition from double-positive to single-positive stage and predisposes thymocytes to malignant transformation. Blood **109:**5463–5472.
21. **Haines, B. B., C. J. Ryu, S. Chang, A. Protopopov, A. Luch, Y. H. Kang, D. D. Draganov, M. F. Fragoso, S. G. Paik, H. J. Hong, R. A. DePinho, and J. Chen.** 2006. Block of T cell development in P53-deficient mice accelerates development of lymphomas with characteristic RAG-dependent cytogenetic alterations. Cancer Cell **9:**109–120.
22. **Haks, M. C., P. Krimpenfort, J. H. van den Brakel, and A. M. Kruisbeek.** 1999. Pre-TCR signaling and inactivation of p53 induces crucial cell survival pathways in pre-T cells. Immunity **11:**91–101.
23. **Harada, N., Y. Tamai, T. Ishikawa, B. Sauer, K. Takaku, M. Oshima, and M. M. Taketo.** 1999. Intestinal polyposis in mice with a dominant stable mutation of the beta-catenin gene. EMBO J. **18:**5931–5942.
24. **Harris, S. L., and A. J. Levine.** 2005. The p53 pathway: positive and negative feedback loops. Oncogene **24:**2899–2908.
25. **He, T. C., A. B. Sparks, C. Rago, H. Hermeking, L. Zawel, L. T. da Costa, P. J. Morin, B. Vogelstein, and K. W. Kinzler.** 1998. Identification of c-MYC as a target of the APC pathway. Science **281:**1509–1512.
26. **Honeycutt, K. A., and D. R. Roop.** 2004. c-Myc and epidermal stem cell fate determination. J. Dermatol. **31:**368–375.
27. **Jiang, D., M. J. Lenardo, and J. C. Zuniga-Pflucker.** 1996. p53 prevents maturation to the CD4+CD8+ stage of thymocyte differentiation in the absence of T cell receptor rearrangement. J. Exp. Med. **183:**1923–1928.
28. **Kinzler, K. W., and B. Vogelstein.** 1996. Lessons from hereditary colorectal cancer. Cell **87:**159–170.
29. **Kirstetter, P., K. Anderson, B. T. Porse, S. E. Jacobsen, and C. Nerlov.** 2006. Activation of the canonical Wnt pathway leads to loss of hematopoietic stem cell repopulation and multilineage differentiation block. Nat. Immunol. **7:**1048–1056.
30. **Lee, G. S., M. B. Neiditch, S. S. Salus, and D. B. Roth.** 2004. RAG proteins shepherd double-strand breaks to a specific pathway, suppressing error-prone repair, but RAG nicking initiates homologous recombination. Cell **117:**171–184.
31. **Li, G. C., H. Ouyang, X. Li, H. Nagasawa, J. B. Little, D. J. Chen, C. C. Ling, Z. Fuks, and C. Cordon-Cardo.** 1998. Ku70: a candidate tumor suppressor gene for murine T cell lymphoma. Mol. Cell **2:**1–8.
32. **Liao, M. J., X. X. Zhang, R. Hill, J. Gao, M. B. Qumsiyeh, W. Nichols, and T. Van Dyke.** 1998. No requirement for V(D)J recombination in p53-deficient thymic lymphoma. Mol. Cell. Biol. **18:**3495–3501.
33. **Liyanage, M., A. Coleman, S. du Manoir, T. Veldman, S. McCormack, R. B. Dickson, C. Barlow, A. Wynshaw-Boris, S. Janz, J. Wienberg, M. A. Ferguson-Smith, E. Schrock, and T. Ried.** 1996. Multicolour spectral karyotyping of mouse chromosomes. Nat. Genet. **14:**312–315.
34. **Lo Celso, C., D. M. Prowse, and F. M. Watt.** 2004. Transient activation of beta-catenin signalling in adult mouse epidermis is sufficient to induce new hair follicles but continuous activation is required to maintain hair follicle tumours. Development **131:**1787–1799.
35. **Mallette, F. A., M. F. Gaumont-Leclerc, and G. Ferbeyre.** 2007. The DNA damage signaling pathway is a critical mediator of oncogene-induced senescence. Genes Dev. **21:**43–48.
36. **Malumbres, M., I. Pérez De Castro, M. I. Hernández, M. Jiménez, T. Corral, and A. Pellicer.** 2000. Cellular response to oncogenic Ras involves induction of the Cdk4 and Cdk6 inhibitor p15^{INK4b}. Mol. Cell. Biol. **20:**2915–2925.
37. **Michaelson, J. S., and P. Leder.** 2001. Beta-catenin is a downstream effector of Wnt-mediated tumorigenesis in the mammary gland. Oncogene **20:**5093–5099.
38. **Michaloglou, C., L. C. Vredeveld, M. S. Soengas, C. Denoyelle, T. Kuilman, C. M. van der Horst, D. M. Majoor, J. W. Shay, W. J. Mooi, and D. S. Peeper.** 2005. BRAFE600-associated senescence-like cell cycle arrest of human naevi. Nature **436:**720–724.
39. **Mulroy, T., J. A. McMahon, S. J. Burakoff, A. P. McMahon, and J. Sen.** 2002. Wnt-1 and Wnt-4 regulate thymic cellularity. Eur. J. Immunol. **32:**967–971.
40. **Mulroy, T., Y. Xu, and J. M. Sen.** 2003. Beta-catenin expression enhances generation of mature thymocytes. Int. Immunol. **15:**1485–1494.
41. **Nacht, M., and T. Jacks.** 1998. V(D)J recombination is not required for the development of lymphoma in p53-deficient mice. Cell Growth Differ. **9:**131–138.
42. **Okamura, R. M., M. Sigvardsson, J. Galceran, S. Verbeek, H. Clevers, and R. Grosschedl.** 1998. Redundant regulation of T cell differentiation and TCRalpha gene expression by the transcription factors LEF-1 and TCF-1. Immunity **8:**11–20.
43. **Pinto, D., and H. Clevers.** 2005. Wnt control of stem cells and differentiation in the intestinal epithelium. Exp. Cell Res. **306:**357–363.
44. **Polakis, P.** 2000. Wnt signaling and cancer. Genes Dev. **14:**1837–1851.
45. **Pongracz, J. E., S. M. Parnell, T. Jones, G. Anderson, and E. J. Jenkinson.** 2006. Overexpression of ICAT highlights a role for catenin-mediated canonical Wnt signalling in early T cell development. Eur. J. Immunol. **36:**2376–2383.
46. **Reschly, E. J., C. Spaulding, T. Vilimas, W. V. Graham, R. L. Brumbaugh, I. Aifantis, W. S. Pear, and B. L. Kee.** 2006. Notch1 promotes survival of E2A-deficient T cell lymphomas through pre-T cell receptor-dependent and -independent mechanisms. Blood **107:**4115–4121.
47. **Reya, T., A. W. Duncan, L. Ailles, J. Domen, D. C. Scherer, K. Willert, L. Hintz, R. Nusse, and I. L. Weissman.** 2003. A role for Wnt signalling in self-renewal of haematopoietic stem cells. Nature **423:**409–414.
48. **Ridgeway, A. G., J. McMenamin, and P. Leder.** 2006. P53 levels determine outcome during beta-catenin tumor initiation and metastasis in the mammary gland and male germ cells. Oncogene **25:**3518–3527.
49. **Rogakou, E. P., C. Boon, C. Redon, and W. M. Bonner.** 1999. Megabase chromatin domains involved in DNA double-strand breaks in vivo. J. Cell Biol. **146:**905–916.
50. **Rooney, S., F. W. Alt, J. Sekiguchi, and J. P. Manis.** 2005. Artemis-independent functions of DNA-dependent protein kinase in Ig heavy chain class switch recombination and development. Proc. Natl. Acad. Sci. USA **102:**2471–2475.
51. **Rooney, S., J. Sekiguchi, S. Whitlow, M. Eckersdorff, J. P. Manis, C. Lee, D. O. Ferguson, and F. W. Alt.** 2004. Artemis and p53 cooperate to suppress oncogenic N-myc amplification in progenitor B cells. Proc. Natl. Acad. Sci. USA **101:**2410–2415.
52. **Scheller, M., J. Huelsken, F. Rosenbauer, M. M. Taketo, W. Birchmeier, D. G. Tenen, and A. Leutz.** 2006. Hematopoietic stem cell and multilineage defects generated by constitutive beta-catenin activation. Nat. Immunol. **7:**1037–1047.
53. **Schilham, M. W., A. Wilson, P. Moerer, B. J. Benaissa-Trouw, A. Cumano, and H. C. Clevers.** 1998. Critical involvement of Tcf-1 in expansion of thymocytes. J. Immunol. **161:**3984–3991.
54. **Serinsoz, E., M. Neusch, G. Busche, R. Wasielewski, H. Kreipe, and O. Bock.** 2004. Aberrant expression of beta-catenin discriminates acute myeloid leukaemia from acute lymphoblastic leukaemia. Br. J. Haematol. **126:**313–319.
55. **Serrano, M., A. W. Lin, M. E. McCurrach, D. Beach, and S. W. Lowe.** 1997. Oncogenic ras provokes premature cell senescence associated with accumulation of p53 and p16INK4a. Cell **88:**593–602.
56. **Sharpless, N. E., and R. A. DePinho.** 2005. Cancer: crime and punishment. Nature **436:**636–637.
57. **Shelton, D. N., E. Chang, P. S. Whittier, D. Choi, and W. D. Funk.** 1999. Microarray analysis of replicative senescence. Curr. Biol. **9:**939–945.
58. **Sicinska, E., I. Aifantis, L. Le Cam, W. Swat, C. Borowski, Q. Yu, A. A. Ferrando, S. D. Levin, Y. Geng, H. von Boehmer, and P. Sicinski.** 2003. Requirement for cyclin D3 in lymphocyte development and T cell leukemias. Cancer Cell **4:**451–461.
59. **Staal, F. J., J. Meeldijk, P. Moerer, P. Jay, B. C. van de Weerdt, S. Vainio, G. P. Nolan, and H. Clevers.** 2001. Wnt signaling is required for thymocyte development and activates Tcf-1 mediated transcription. Eur. J. Immunol. **31:**285–293.
60. **Talora, C., S. Cialfi, C. Oliviero, R. Palermo, M. Pascucci, L. Frati, A. Vacca, A. Gulino, and I. Screpanti.** 2006. Cross talk among Notch3, pre-TCR, and Tal1 in T-cell development and leukemogenesis. Blood **107:**3313–3320.
61. **Tetsu, O., and F. McCormick.** 1999. Beta-catenin regulates expression of cyclin D1 in colon carcinoma cells. Nature **398:**422–426.
62. **van Meerwijk, J. P., H. Bluthmann, and M. Steinmetz.** 1990. T-cell specific rearrangement of T-cell receptor beta transgenes in mice. EMBO J. **9:**1057–1062.
63. **von Boehmer, H.** 2005. Unique features of the pre-T-cell receptor alpha-chain: not just a surrogate. Nat. Rev. Immunol. **5:**571–577.
64. **Weerkamp, F., J. J. van Dongen, and F. J. Staal.** 2006. Notch and Wnt signaling in T-lymphocyte development and acute lymphoblastic leukemia. Leukemia **20:**1197–1205.
65. **Xu, Y., D. Banerjee, J. Huelsken, W. Birchmeier, and J. M. Sen.** 2003. Deletion of beta-catenin impairs T cell development. Nat. Immunol. **4:**1177–1182.
66. **Xu, Y., and J. Sen.** 2003. Beta-catenin expression in thymocytes accelerates thymic involution. Eur. J. Immunol. **33:**12–18.
67. **Yu, Q., and J. M. Sen.** 2007. Beta-catenin regulates positive selection of thymocytes but not lineage commitment. J. Immunol. **178:**5028–5034.
68. **Zhu, C., K. D. Mills, D. O. Ferguson, C. Lee, J. Manis, J. Fleming, Y. Gao, C. C. Morton, and F. W. Alt.** 2002. Unrepaired DNA breaks in p53-deficient cells lead to oncogenic gene amplification subsequent to translocations. Cell **109:**811–821.